

# Spin-charge separation in two-component Bose-gases

A. Kleine,<sup>1</sup> C. Kollath,<sup>2</sup> I.P. McCulloch,<sup>1</sup> T. Giamarchi,<sup>2</sup> and U. Schollwöck<sup>1</sup>

<sup>1</sup>*Institute for Theoretical Physics C, RWTH Aachen, D-52056 Aachen, Germany*

<sup>2</sup>*DPMC-MaNEP, University of Geneva, 24 Quai Ernest-Ansermet, CH-1211 Geneva, Switzerland*

(Dated: February 1, 2008)

We show that one of the key characteristics of interacting one-dimensional electronic quantum systems, the separation of spin and charge, can be observed in a two-component system of bosonic ultracold atoms even close to a competing phase separation regime. To this purpose we determine the real-time evolution of a single particle excitation and the single-particle spectral function using density-matrix renormalization group techniques. Due to efficient bosonic cooling and good tunability this setup exhibits very good conditions for observing this strong correlation effect. In anticipation of experimental realizations we calculate the velocities for spin and charge perturbations for a wide range of parameters.

One of the most exciting recent events is the ever-growing interplay between previously disconnected fields of physics, such as quantum optics and condensed matter physics. In particular, cold atomic systems have opened the way to engineer strongly interacting quantum many-body systems of unique purity. The unprecedented control over interaction strength and dimensionality allows the realization of “quantum simulators” where fundamental but hard to analyze phenomena in strongly correlated systems could be observed and controlled. Examples are the observation of superfluid to Mott insulator transition for Bose gases [1] and the fermionization of strongly interacting one dimensional bosons [2, 3].

Among interacting systems, the physics depends very strongly on the dimensionality. In one-dimensional systems the interactions play a major role and lead to drastically different physics than for their higher dimensional counterpart. Typically, interactions in one-dimensional systems lead to a Luttinger liquid state where the excitations of the system are collective excitations [4]. The importance of such a state for a large variety of experimental devices in condensed matter has led to a hunt to observe its properties. A remarkable consequence of such a state is the absence of single particle excitations. This means that a quantum particle, that would normally carry both charge and spin degrees of freedom, fractionalizes into two different collective excitations, a spin and a charge excitation. Such a fractionalization of a single particle excitation is the hallmark of collective effects caused by interactions. However, just as detecting fractional excitations in the case of the quantum hall effect is difficult [5], observing spin-charge separation has proven elusive despite several experimental attempts [6, 7, 8]. So far, the best experimental evidence is provided by tunneling between quantum wires where interference effects are due to the existence of two different velocities [9]. However, in these systems it is hard to quantify or to tune the interaction between the particles which causes the collective effects. Since control of the interaction is a routing procedure in ultracold gases, the possible realization of the phenomenon of spin charge separation has

also been discussed in the context of cold fermionic gases [10, 11, 12, 13] and strongly interacting bosonic gases [14].

However, proposals to observe spin-charge separation in ultracold fermionic gases are still plagued by the currently quite high temperatures in such systems. A much better setup to test for spin-charge separation would be two-component Bose gases, for example using the  $|F = 2, m_F = -1\rangle$  and the  $|F = 1, m_F = 1\rangle$  hyperfine states of  $^{87}\text{Rb}$  [15, 16]. Experimentally, this system retains the advantages of the fermionic ultracold atom setup while allowing for much lower temperatures due to the more efficient cooling techniques available for bosons. However, theoretical studies [17, 18] for one-dimensional systems predict that close to the experimentally accessible parameter regime of almost equal inter- and intra-species interaction strength phase separation occurs. This is the remaining potential experimental complication in the setup.

In this work we demonstrate the phenomenon of spin-charge separation in the experimentally relevant parameter regime, allowing to use this system to unambiguously test for spin-charge separation. We calculate both the real-time evolution of a single particle excitation and the dynamical single particle spectral function of the two-component bosonic systems. We show that both these quantities demonstrate the separation of a single-particle excitation into spin and charge. We further determine the velocity of spin and charge and the Luttinger parameters for experimentally relevant parameter regimes. To perform the calculations we use variants of the density matrix renormalization group method (DMRG) [19, 20]. The numerical treatment is necessary to obtain reliable predictions for experimental realizations, due to the close proximity of this regime to phase separation.

A one-dimensional two-component Bose gas in an optical lattice [21] can be described by the two-component

Bose-Hubbard model

$$H = -J \sum_{j,\nu} \left( b_{j+1,\nu}^\dagger b_{j,\nu} + h.c. \right) + \sum_{j,\nu} \frac{U_\nu \hat{n}_{j,\nu} (\hat{n}_{j,\nu} - 1)}{2} + U_{12} \sum_j \hat{n}_{j,1} \hat{n}_{j,2} + \sum_{j,\nu} \varepsilon_{j,\nu} \hat{n}_{j,\nu} \quad (1)$$

Here  $j$  is the site index and  $\nu = 1, 2$  labels the two different hyperfine states of the system,  $b$  and  $b^\dagger$  are the annihilation and creation operators and  $\hat{n}$  is the number operator. The first term models the kinetic energy of the atoms. The intra-species interaction is described by the  $U_\nu$  term. We use  $U := U_1 = U_2$  as it is approximately realized for commonly used hyperfine states of  $^{87}\text{Rb}$  [22]. The inter-species interaction is given by the  $U_{12}$  term and the last term describes external potentials. In the following we use the dimensionless parameters  $u = U/J$  and  $u_{12} = U_{12}/J$ . We define the ‘charge’ density  $n_{j,c} = n_{j,1} + n_{j,2}$  and the ‘spin’ density  $n_{j,s} = n_{j,1} - n_{j,2}$ . We focus on systems with average filling  $n = \sum_j n_{j,1}/L = \sum_j n_{j,2}/L$  smaller than one particle per site and parameter regimes up to close to the transition to the phase separation (approximately  $u_{12} \approx u$  [18]). Here  $L$  is the number of sites in the system.

In a superfluid phase away from the transition to phase separation the low energy physics can be approximated by a density-phase representation of the bosons as used in the bosonization method [4]. In this representation the Hamiltonian is totally separated into one part for the charge and one for the spin degrees of freedom. The physics is fully determined by the velocities  $v_{c,s}$  and the so-called Luttinger parameters  $K_{c,s}$  for spin (s) and charge (c). Therefore the separation of a single particle excitation into spin and charge excitations is expected. The parameters of two interacting species of bosons can be related to the parameters  $K$  and  $v_0$  for the single species case [23] by

$$\begin{aligned} v_{c,s} &= v_0 \sqrt{1 \pm (g_{12}K)/(\pi v_0)} \\ \text{and } K_{c,s} &= K / \sqrt{1 \pm (g_{12}K)/(\pi v_0)}. \end{aligned} \quad (2)$$

Here  $g_{12}$  is the interspecies interaction strength in the continuous model. In the limit of small interactions, the single species parameters  $K$  and  $v_0$  can be directly related to the Bose-Hubbard Hamiltonian Eq. (1) [4]. For higher values of the interaction strength the relation even for the single species situation is unknown, and has to be determined numerically [24]. For large values of the inter-species interaction of the order of the intra-species interaction the system approaches the transition to phase separation and the bosonization approach becomes a priori inaccurate.

Snapshots of the real time-evolution of a single particle excitation in a two-component bosonic system are shown in Fig. 1. The single particle excitation at time  $t = 0$  is prepared by the application of the creation operator of one species, say 1, on site  $L/2$  to the ground state  $|\psi_0\rangle$ , i.e.  $b_{L/2,1}^\dagger |\psi_0\rangle$ . The resulting sharp peaks in

the density distributions are shown in Fig. 1 (a). For  $t > 0$  the time-evolution of the single particle excitation is calculated using the adaptive time-dependent DMRG [25, 26]. The time-evolution is performed using a Krylov algorithm [27] in a matrix product state basis with a fixed error bound for each timestep of the order of  $\|\Psi(t + \Delta t) - \exp[-iH\Delta t]\Psi(t)\|^2 < 10^{-5}$ . The stepsize  $\Delta t = 0.2$  and 6 to 10 Krylov vectors were used resulting in Hilbert spaces with a local dimension of a few thousand states. As can be seen in the snapshots in Fig. 1 the initial single particle excitation splits up into two counter propagating density waves. Due to their different spin and charge velocities, after a period of time a clear separation of the density waves is seen (cf. Fig. 1 (c)) [41].

Additionally to the time-evolution of a single particle excitation, we obtained the single particle spectral function  $A_\nu(q, \omega) = \frac{1}{\pi} \Im \langle b_{q,\nu}^\dagger \frac{1}{H + \omega + i\eta - E_0} b_{q,\nu} \rangle$  as shown in Fig. 2. For fermions this function is known to exhibit two peaks at the spin and charge excitation energies [28, 29], showing a direct signature of the spin-charge separation. For the bosons computing this spectral function is more involved and up to very recently it was only derived for a single component bosonic system [30, 31, 32]. An expression for the correlation functions which allow to obtain the single-particle correlation function within the bosonization treatment for a two-component bosonic system was derived in [33]. Power law singularities at  $qv_{c,s}$  are obtained with respective exponents  $1/4K_{c,s} + 1/2K_{s,c} - 1$ . For the values of the Luttinger parameters (as shown in Fig. 2) one thus expects two divergent peaks. We show in Fig. 2 the full spectral function for our microscopic model, as calculated numerically using a matrix product state generalization of the correction vector method [31, 34]. Our results show clearly the appearance of the two separated peaks, the lower representing the spin and the upper the charge excitation branch [42]. Thus both the real time evolution of a single particle function and the single particle spectral function show clear signatures of separation of spin and charge.

To observe the separation of spin and charge excitations experimentally in a system of ultracold bosons, knowledge of the spin and charge velocities is indispensable. We therefore determined the velocities for a wide range of parameters. This was done calculating the time-evolution of a small spin and charge density perturbation respectively. The density perturbation was created at time  $t = 0$  applying an external potential of Gaussian form  $\varepsilon_{\nu,j} = \varepsilon_0 \exp\left(-\frac{(j-j_0)^2}{2\sigma_j}\right)$  where  $\nu = c, s$ . At time  $t = 0$  the potential is switched off and the time-evolution of the density perturbation is calculated. The errors in the obtained velocities are of the order of  $0.01aJ/\hbar$  for small  $u_{12}$  and increase with larger  $u_{12}$ .

In Fig. 3 we show the dependence of the velocities

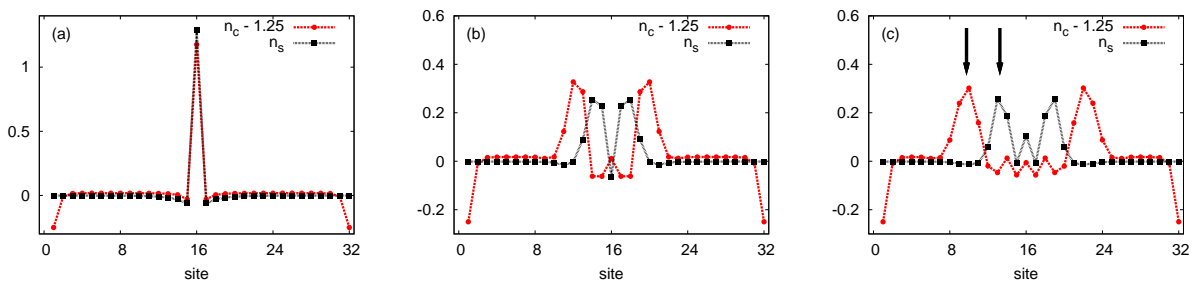


FIG. 1: (Color online) Snapshots of the time-evolution of the charge and spin density distribution of a single particle excitation created at time  $t = 0\hbar/J$ ; (a) at time  $t = 0\hbar/J$ , (b) at time  $t = 1.5\hbar/J$  and (c) at time  $t = 2.5\hbar/J$ . The system parameters were  $n_{1,2} = 0.625$ ,  $u = 3$ ,  $u_{12} = 2.1$ . The charge density is shifted by 1.25 for better visibility. The arrows in (c) mark the clear separation of the charge and the spin density waves.

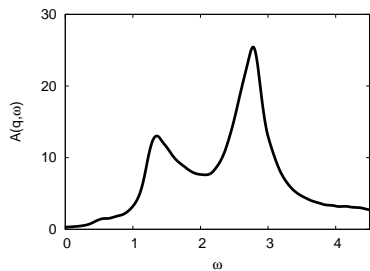


FIG. 2: One-particle spectral function at momentum  $q = 20/65\pi/a$ . Two peaks corresponding to the spin and the charge excitation can be distinguished. The following parameters were used  $n = 0.625$ ,  $u = 3$ ,  $u_{12} = 2.1$  on a system with  $L = 64$  sites and a broadening  $\eta = 0.1$ . Here  $a$  is the lattice spacing.

on the inter-species interaction for two different values of the parameter  $\gamma = u/(2n_c)$ . For both parameter regimes, the charge velocity increases with increasing interaction whereas the spin velocity decreases. For a vanishing inter-species interaction it was shown in [24] that for  $\gamma < 1$  the bosonization and the solution of the exactly solvable Lieb-Liniger model agree approximately with the velocities in the Bose-Hubbard model. In Fig. 3 (a) we find for  $\gamma \approx 1.1$  very good agreement with the analytical solutions even up to strong inter-species interaction strength  $u_{12}$  close to phase separation. For  $\gamma \approx 2.4$  [cf. Fig. 3 (b)] even for vanishing interspecies interaction the deviations from the direct relation between the parameters in the Bose-Hubbard model are considerable (cf. [24]). However, we find that the dependence of the velocities on the interspecies interaction strength via Eq. (2) is still a good approximation correcting by the numerically determined value for  $v_0$  and  $K$ . This holds even up to close to the regime of phase separation, i.e.  $u_{12} \approx u$  where the difference in the velocities is maximal. However, for  $u_{12} \approx u$  the results for the spin velocity start to deviate for both values of  $\gamma$ .

In Fig. 4 we show for two different fixed inter-species interaction strengths the dependence of the velocities on the density. The charge and the spin velocities rise with increasing background charge density. (Note, even at  $n_c = 1$  the system is in the superfluid regime.) The increase of the velocities is described to good accuracy using the analytical form Eq. (2), provided we use numerically obtained values of  $K$  and  $v_0$ . For large  $u_{12}$  and small  $n_c$  the results for the velocities from DRMG, in particular the spin velocity, deviate considerably from Eq. (2), showing that the approximate relation cannot be used in this regime. Note that in this regime the extraction of the spin velocity from the real-time evolution becomes also more involved since the spin perturbation shows a strong spreading in space (cf. [35]). At the timescales over which we calculated the velocity, the left- and the right-moving spin perturbations are not yet fully separated and show strong amplitude damping. Our finding of the dependencies can be used to predict the velocities for experimentally interesting parameter regimes.

In recent experiments for the preparation of a mixture of two bosonic components in optical lattices mostly two hyperfine states of  $^{87}\text{Rb}$  are used, e.g. the  $|F = 2, m_F = -1\rangle$  and the  $|F = 1, m_F = 1\rangle$  hyperfine states. The intra-species scattering lengths are  $a_2 = 91.28a_B$  and  $a_1 = 100.4a_B$  [22], respectively where  $a_B$  is the Bohr radius. For these states the inter-species scattering length is of the same order of magnitude as the intra-species scattering length and can be tuned about 20% using a Feshbach resonance [15, 16]. Thereby the experimental parameters are close to the competing phase separation regime. These mixtures can be confined to one-dimensional structures using strongly anisotropic lattices [2, 3, 36, 37]. The most intuitive observation of the phenomenon of spin-charge separation in these systems is to generate a single particle excitation and then follow the evolution of the excitation in real time. This can be done measuring the spin-resolved density over a certain region. The creation of a single particle excitation can

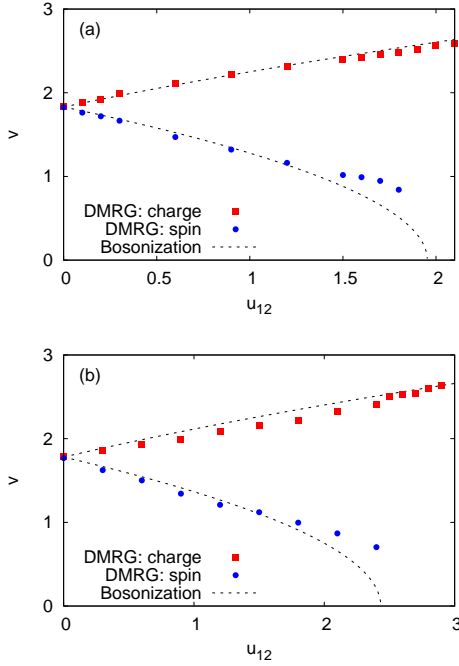


FIG. 3: (Color online) Dependence of the charge and spin velocity on the interparticle interaction strength for (a)  $u_{12} = 2$  and  $n \approx 0.88$  and (b)  $u_{12} = 3$  and  $n = 0.63$ . A comparison of analytical results (line, see text) and numerical DMRG results (symbol) is shown. The velocities are measured in units  $aJ/\hbar$ . Note that the errors of the DMRG results increase close to  $u_{12} \approx u$ .

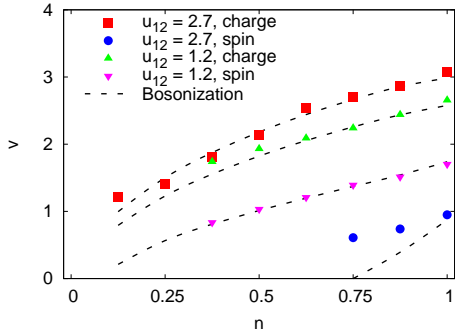


FIG. 4: (Color online) Dependence of the charge and spin velocity on the charge background density, comparison analytical results of bosonization and numerical DMRG results. The parameters used are (a)  $u = 3$ ,  $u_{12} = 1.2$  and (b)  $u = 3$ ,  $u_{12} = 2.7$ .

be done e.g. using outcoupling of single particles by the application of a magnetic field gradient for addressability and a microwave field [38, 39, 40][43]. The efficiency of such a technique for generating single particle excitations was demonstrated [39] using a cavity. The microwave field could be chosen to couple the  $|F = 1, m_F = 1\rangle$  hy-

perfine state to e.g. the  $|F = 2, m_F = 2\rangle$ . This has the advantage that scattering with the  $|F = 1, m_F = 1\rangle$  state are suppressed. The measurement of the density resolved over a region of approximately 10 lattice sites can then be performed using again the magnetic field gradient to get an unambiguous signal. In an array of one-dimensional tubes the broadening of the signal caused by the trapping potential could be suppressed by preparing most of the tubes in a Mott-insulating state as shown in [12].

We would like to thank J.S. Caux, S. Fölling, M. Köhl, and B. Paredes for fruitful discussions. AK and US acknowledge support by the DFG and CK and TG by the Swiss National Fund under MaNEP and Division II and the CNRS. CK thanks the Institut Henri Poincaré for its hospitality during the final part of the work.

- 
- [1] M. Greiner *et al.*, Nature **415**, 39 (2002).
  - [2] B. Paredes *et al.*, Nature **429**, 277 (2004).
  - [3] T. Kinoshita, T. Wenger, and D. S. Weiss, Science **305**, 1125 (2004).
  - [4] T. Giamarchi, *Quantum Physics in One Dimension* (Oxford University Press, 2004).
  - [5] C. Glattli, in *High Magnetic Fields: Applications in Condensed Matter Physics and Spectroscopy*, edited by C. Berthier *et al.* (Springer-Verlag, Berlin, 2002), p. 1.
  - [6] P. Segovia *et al.*, Nature **402**, 504 (1999).
  - [7] T. Lorenz *et al.*, Nature **418**, 614 (2002).
  - [8] C. Kim *et al.*, Phys. Rev. Lett. **77**, 4054 (1996).
  - [9] O. M. Auslaender *et al.*, Science **308**, 88 (2005).
  - [10] A. Recati *et al.*, Phys. Rev. Lett. **90**, 020401 (2003).
  - [11] L. Kecke, H. Grabert, and W. Hausler, Phys. Rev. Lett. **94**, 176802 (2005),
  - [12] C. Kollath, U. Schollwöck, and W. Zwerger, Phys. Rev. Lett. **95**, 176401 (2005).
  - [13] C. Kollath and U. Schollwöck, New J. Phys. **8**, 220 (2006),
  - [14] B. Paredes and J. I. Cirac, Phys. Rev. Lett. **90**, 150402 (2003).
  - [15] M. Erhard *et al.*, **69**, 032705 (2004),
  - [16] A. Widera *et al.*, Phys. Rev. Lett. **92**, 160406 (2004),
  - [17] M. A. Cazalilla and A. F. Ho, Phys. Rev. Lett. **91**, 150403 (2003).
  - [18] T. Mishra, R. V. Pai, and B. P. Das, cond-mat/0610121 (2006).
  - [19] S. R. White, Phys. Rev. Lett. **69**, 2863 (1992).
  - [20] U. Schollwöck, Rev. Mod. Phys. **77**, 259 (2005).
  - [21] D. Jaksch *et al.*, Phys. Rev. Lett. **81**, 3108 (1998).
  - [22] A. Widera *et al.*, New J. Phys. **8**, 152 (2006).
  - [23] E. Orignac and T. Giamarchi, Phys. Rev. B **57**, 11713 (1998).
  - [24] C. Kollath *et al.*, Phys. Rev. A **71**, 053606 (2005).
  - [25] A. J. Daley *et al.*, J. Stat. Mech.: Theor. Exp. **P04005** (2004).
  - [26] S. R. White and A. E. Feiguin, Phys. Rev. Lett. **93**, 076401 (2004).
  - [27] M. Hochbruck and C. Lubich, SIAM J. Numer. Anal. **34**, 1911 (1997).
  - [28] V. Meden and K. Schönhammer, Phys. Rev. B **46**, 15753

- (1992).
- [29] J. Voit, Phys. Rev. B **47**, 6740 (1993).
  - [30] F. D. M. Haldane, Phys. Rev. Lett. **47**, 1840 (1981).
  - [31] T. D. Kühner and S. R. White, Phys. Rev. B **60**, 335 (1999).
  - [32] J.-S. Caux and P. Calabrese, cond-mat/0603654 (2006).
  - [33] A. Iucci, G. A. Fiete, and T. Giamarchi, Phys. Rev. B **75**, 205116 (2007),
  - [34] A. Friedrich *et al.*, Phys. Rev. B **75**, 094414 (2007).
  - [35] M. Polini and G. Vignale, cond-mat/0702466 (2007).
  - [36] H. Moritz *et al.*, Phys. Rev. Lett. **91**, 250402 (2003).
  - [37] B. L. Tolra *et al.*, Phys. Rev. Lett. **92**, 190401 (2004),
  - [38] I. Bloch, T. Hänsch, and T. Esslinger, Nature **403**, 166 (2000).
  - [39] A. Öttl *et al.*, Phys. Rev. Lett. **95**, 090404 (2005).
  - [40] S. Fölling *et al.*, Phys. Rev. Lett. **97**, 060403 (2006).
  - [41] The remaining interaction between the spin and the charge degrees of freedom for short times can cause small additional structures beside the main peaks in the density wave profiles [Fig. 1 (c)].
  - [42] Given the relatively large value of  $q$  that we use and the band curvature that exists in the microscopic model it is difficult to quantitatively compare the position of the peaks to the bosonization result  $u_{c,s}q$ , valid for small  $q$  or a strictly linear dispersion relation.
  - [43] The magnetic field gradient can be applied since the two hyperfine states have approximately the same magnetic moment.